

# Determination of energy barriers to rotation and absolute conformations of thermally interconvertible 5,5-dimethyl-3-(*o*-aryl)-2,4-oxazolidinedione enantiomers

Öznur Demir Ordu and İlkur Doğan\*

Boğaziçi University, Chemistry Department, Bebek, 34342 Istanbul, Turkey

Received 21 November 2003; accepted 22 December 2003

**Abstract**—The activation barriers for the interconversion between the enantiomers of 5,5-dimethyl-3-(*o*-aryl)-2,4-oxazolidinediones ( $M \rightleftharpoons P$ ) have been determined by temperature dependent NMR and by enantioresolution on chiral sorbents via HPLC. The activation barriers were found to increase linearly with the size of the van der Waals radii of the *ortho*-halogen substituents. The enantiomers of the *o*-iodo derivative were microreparatively enriched on a Chiralpak AD column, leading to the determination of its barrier to rotation via thermal racemization and resulting in the assignments of conformations in the presence of the optically active chiral auxiliary (*S*)-(+)-1-(9-anthryl)-2,2,2-trifluoro ethanol [(*S*)-TFAE].

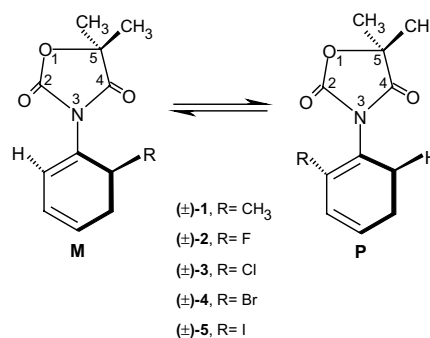
© 2004 Elsevier Ltd. All rights reserved.

## 1. Introduction

Compounds bearing an oxazolidine ring are of considerable interest due to their presence in a number of biologically active synthetic products,<sup>1,2</sup> and their utility as directing groups in asymmetric synthesis.<sup>3,4</sup> The 5,5-dimethyl-2,4-oxazolidinedione ring is present in some antidiabetic drugs,<sup>2</sup> and anticonvulsants.<sup>5</sup> Introducing an *o*-substituted phenyl ring to the oxazolidine ring on the nitrogen atom brings dissymmetry and makes these compounds axially chiral due to restricted rotation around the  $C_{\text{aryl}}-N_{\text{sp}^2}$  single bond, which gives an enantiomeric pair of atropisomers.<sup>6</sup>

In our previous work on (5*S*)-methyl-3-(*o*-aryl)-2,4-oxazolidinediones, which were obtained in unequal compositions of the two diastereomers,<sup>7</sup> we found that the 5-methyl group had enough spacial proximity to the *ortho* methyl or hydrogen atom that enabled us to determine the absolute conformation of the major and the minor diastereomers. Starting from this set of compounds, in this study we determine the barrier to rotation of the analogous enantiomers (Scheme 1) either by enantioresolution of the racemic compounds on chiral sorbents via HPLC or by temperature dependent NMR and comment on the absolute conformations of

the two enantiomers by the help of the chiral auxiliary (*S*)-(+)-1-(9-anthryl)-2,2,2-trifluoro ethanol [(*S*)-TFAE] and by comparison of what we have found in the previous work for the (5*S*)-methyl-3-(*o*-aryl)-2,4-oxazolidinediones.



Scheme 1. The synthesized compounds.

## 2. Results and discussion

### 2.1. <sup>1</sup>H and <sup>13</sup>C NMR

5,5-Dimethyl-3-(*o*-aryl)-2,4-oxazolidinedione derivatives (Scheme 1) were synthesized by the reaction of *o*-aryl isocyanates with ethyl  $\alpha$ -hydroxyisobutyrate in the

\* Corresponding author. Tel.: +90-212-358-1540; fax: +90-212-287-2467; e-mail: [dogan@boun.edu.tr](mailto:dogan@boun.edu.tr)

presence of sodium metal in toluene.<sup>7</sup> The rotational isomers of the synthesized compounds are enantiomeric and expected to exhibit identical NMR spectra in an achiral solvent. However, the methyl protons on the C-5 position of the heterocyclic ring, because of the presence of a C<sub>aryl</sub>-N<sub>sp<sup>2</sup></sub> chiral axis, are diastereotopically related, and should be, in principle, magnetically nonequivalent provided that the rate of internal rotation is slow on the NMR time scale. Analysis of the <sup>1</sup>H NMR spectra did indicate the existence of diastereotopic protons. The two methyl groups on C-5 of the heterocyclic moiety in compounds (±)-**1**, (±)-**3**, (±)-**4**, and (±)-**5** gave two separate singlets with chemical shift differences of 0.02, 0.09, 0.12, and 0.2 ppm, respectively, in C<sub>6</sub>D<sub>6</sub> (Table 1). The diastereotopic methyl groups also exhibited unequal shifts of <sup>13</sup>C nuclei in C<sub>6</sub>D<sub>6</sub>, the shift differences being equal to, 0.7, 0.9, 0.9, and 0.5 ppm, respectively (Table 1). These findings show that the rates of internal rotation are slow on the NMR time scale and confirm the chirality of the compounds in their ground states. For compound (±)-**2**, the *ortho*-fluoro derivative, on the other hand, anisochronous carbon and proton nuclei for the diastereotopic methyl groups were not detected at ordinary probe temperature (30 °C) by NMR. Lowering the probe temperature to -55 °C enabled the observation of these diastereotopic methyl protons.

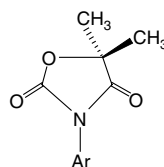
## 2.2. Barriers to rotation

**2.2.1. Temperature dependent NMR.** Activation parameters to hindered rotation around the C–N single bond were determined by temperature dependent NMR spectroscopy for all the synthesized compounds, except for (±)-**5** (for which thermal racemization after micro-preparative enrichment of the enantiomers has been applied). The two magnetically nonequivalent C-5 methyl protons, which were distinguished by NMR at room temperature, became equivalent at higher temperatures (Fig. 1). The kinetic data of the interconversion process were determined using the Eyring equation,<sup>8</sup> and the results are listed in Table 2.

Comparison of the energy barriers of the studied compounds revealed the influence of the relative sizes of the substituents on hindered rotation. As can be seen from Figure 2, the  $\Delta G^\ddagger$  values for the *ortho*-halogen substituted compounds (±)-**2**, (±)-**3**, (±)-**4**, and (±)-**5** were found to increase linearly with the van der Waals radii of the halogens.

Compound (±)-**3** bearing an *o*-chlorine substituent showed a barrier greater than compound (±)-**1** having an *o*-methyl group although the van der Waals radius of

**Table 1.** <sup>1</sup>H and <sup>13</sup>C NMR spectral data for the synthesized compounds in the presence and absence of the optically active auxiliary, (*S*)-TFAE at 30 °C



Compound no	Ar	Medium	<sup>1</sup> H NMR, ppm, C-5 methyl	<sup>1</sup> H NMR, ppm, <i>o</i> -methyl	<sup>13</sup> C NMR, ppm, C-5 methyl
(±)- <b>1</b>	<i>o</i> -Tolyl	C <sub>6</sub> D <sub>6</sub>	1.15 and 1.17 <sup>c</sup>	1.97	23.0, 23.7
		C <sub>6</sub> D <sub>6</sub> +( <i>S</i> )-TFAE <sup>a</sup>	1.06, 1.08, 1.09 <sup>c</sup>	1.88, 1.89 <sup>c</sup>	
(±)- <b>2</b>	<i>o</i> -Fluorophenyl	C <sub>6</sub> D <sub>6</sub>	1.11 <sup>c</sup>	—	23.3
		Acetone- <i>d</i> <sub>6</sub>	1.68 and 1.69 <sup>d,e</sup>	—	—
(±)- <b>3</b>	<i>o</i> -Chlorophenyl	C <sub>6</sub> D <sub>6</sub> +( <i>S</i> )-TFAE <sup>b</sup>	1.05 and 1.06 <sup>c</sup>	—	—
		C <sub>6</sub> D <sub>6</sub>	1.16 and 1.25 <sup>c</sup>	—	22.9, 23.8
(±)- <b>4</b>	<i>o</i> -Bromophenyl	DMSO	1.64 and 1.69 <sup>c</sup>	—	—
		C <sub>6</sub> D <sub>6</sub> +( <i>S</i> )-TFAE <sup>b</sup>	1.10, 1.11, 1.20, 1.21 <sup>c</sup>	—	—
(±)- <b>5</b>	<i>o</i> -Iodophenyl	C <sub>6</sub> D <sub>6</sub>	1.19 and 1.31 <sup>c</sup>	—	22.9, 23.8
		DMSO	1.71 and 1.75 <sup>d</sup>	—	—
		C <sub>6</sub> D <sub>6</sub> +( <i>S</i> )-TFAE <sup>b</sup>	1.12, 1.13, 1.26 <sup>c,f</sup>	—	—
		C <sub>6</sub> D <sub>6</sub>	1.21 and 1.41 <sup>d</sup>	—	21.8, 22.3
		DMSO	1.76 <sup>d</sup>	—	—
		CDCl <sub>3</sub>	1.72 and 1.80 <sup>d</sup>	—	24.1, 24.4
(±)- <b>5</b>	<i>o</i> -Iodophenyl	CDCl <sub>2</sub> CDCl <sub>2</sub>	2.27 and 2.32 <sup>d</sup>	—	—
		C <sub>6</sub> D <sub>6</sub> +( <i>S</i> )-TFAE <sup>a</sup>	0.20, 0.21, 0.39, 0.40 <sup>d</sup>	—	—
		CDCl <sub>3</sub> +TFAE <sup>a</sup>	1.68, 1.69, 1.76, 1.77 <sup>d</sup>	—	—

<sup>a</sup> 1:8 equivalents of (*S*)-TFAE were used.

<sup>b</sup> 1:6 equivalents of (*S*)-TFAE were used.

<sup>c</sup> 200 MHz <sup>1</sup>H NMR spectral data.

<sup>d</sup> 400 MHz <sup>1</sup>H NMR spectral data.

<sup>e</sup> At -55 °C.

<sup>f</sup> A shoulder was observed for the signal at 1.26 ppm.

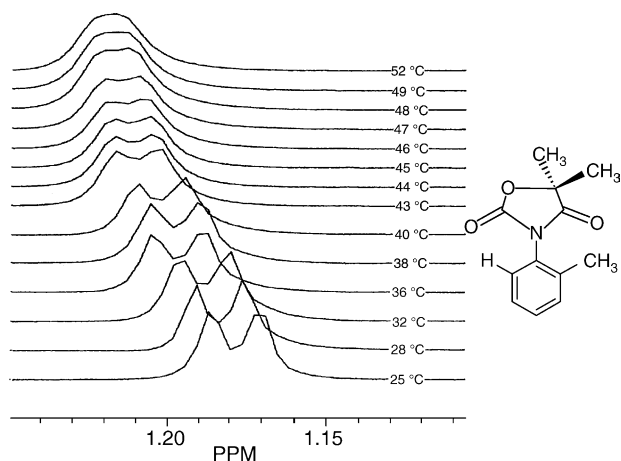


**Figure 1.** The temperature-dependent 200 MHz  $^1\text{H}$  NMR spectrum of the diastereotopic C-5 methyl protons of compound ( $\pm$ )-1.

chlorine is smaller than that for the methyl group. Thus, this difference cannot be explained by consideration of the relative sizes in the planar transition states. Electrostatic repulsion between the lone pairs of carbonyl oxygen and chlorine atom can be expected to make the rotation around C–N single bond more hindered and thus causing a larger barrier for this compound.

**2.2.2. HPLC.** Resolution of the racemic mixtures of interconverting enantiomers was attempted on Chiralcel OD-H and Chiralpak AD columns, packed with cellulose tris-3,5-dimethylphenyl carbamate and amylose tris-3,5-dimethylphenyl carbamate as chiral stationary phases, respectively. On both columns at room temperature, separations of enantiomers were not achieved except for ( $\pm$ )-4 and ( $\pm$ )-5 due to the fact that the barrier to rotation was not sufficiently high to allow. The resolution of enantiomeric peaks was found to be better on the AD column where ( $\pm$ )-4 was separated analytically and ( $\pm$ )-5 micropreparatively in ethanol/hexane (9:1, v/v) as eluent.

In the chromatographic separation of interconverting enantiomers of ( $\pm$ )-5 on a chiral OD-H column, the solvent was found to have an effect on the barrier as has been observed before.<sup>7</sup> When the eluent was 80:20 (v/v)

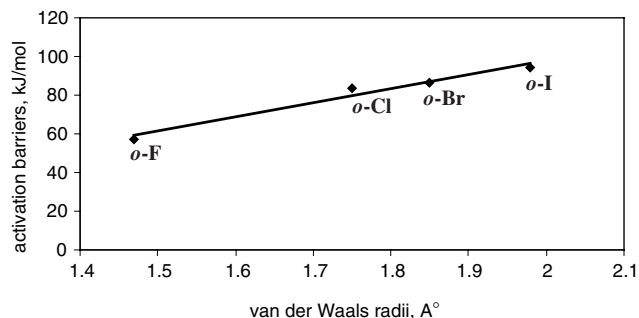


**Figure 2.** The plot of activation barriers versus Van der Waals radii of the *o*-substituted halogens.

hexane/ethanol a series of flow rate and temperature dependent plateaus,<sup>9–11</sup> resulting from on-column racemization were observed (Fig. 3). The interfering ‘plateau’ originated from molecules for which slow racemization took place during elution on the column, whereas the two terminal peaks essentially resulted from molecules that kept their conformation as M or P during the whole resolution process. Increasing the ratio of ethanol in the ethanol/hexane eluent resulted in the disappearance of the plateaus, but decreased the difference between the retention times. A series of flow rate and temperature dependent plateaus were also observed on an AD column for compounds ( $\pm$ )-3 and ( $\pm$ )-4 with eluent composition of ethanol/hexane (1:1, v/v) at a flow rate of 0.3 mL/min, at  $7 \pm 2$  °C. On column racemization can, in fact, be expected for interconvertible enantiomers having barriers about these magnitudes (Table 2) as has been observed before.<sup>10</sup>

For ( $\pm$ )-5 the micropreparative enrichment of the first eluted enantiomer using 90% ethanol/10% hexane as eluent was performed for two purposes: to follow the interconversion between enantiomers in order to obtain the kinetic data (Table 2) of the interconversion process (thermal racemization), which led to the determination of the activation barrier, and, second, to determine the absolute conformations of the enantiomers using (*S*)-TFAE as an optically active auxiliary by NMR as will be described later.

The ethanol solution containing the enriched enantiomer of ( $\pm$ )-5 was kept at a constant temperature (20 °C,

**Table 2.** The kinetic and thermodynamic data for the interconversion process shown in Scheme 1

Compound no	Solvent	T (K)	$k$ ( $\text{s}^{-1}$ )	$\Delta G^\ddagger$ (kJ/mol)
( $\pm$ )-1	$\text{C}_6\text{D}_6$	321 <sup>c</sup>	6.91 <sup>d</sup>	73.49 $\pm$ 0.05 <sup>a</sup>
( $\pm$ )-2	Acetone- $d_6$	247 <sup>c</sup>	3.64 <sup>d</sup>	57.33 $\pm$ 0.05 <sup>b</sup>
( $\pm$ )-3	DMSO- $d_6$	377 <sup>c</sup>	22.97 <sup>d</sup>	83.24 $\pm$ 0.05 <sup>a</sup>
( $\pm$ )-4	DMSO- $d_6$	395 <sup>c</sup>	28.82 <sup>d</sup>	86.62 $\pm$ 0.05 <sup>b</sup>
( $\pm$ )-5	Ethanol/hexane (9:1, v/v)	293 <sup>f</sup>	$1 \times 10^{-4g}$	94.16 $\pm$ 1.31

<sup>a</sup> Determined by 200 MHz NMR instrument.

<sup>b</sup> Determined by 400 MHz NMR instrument.

<sup>c</sup> The coalescence temperature.

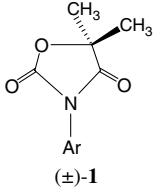
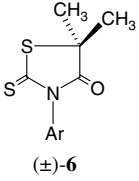
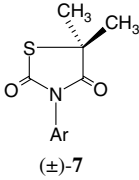
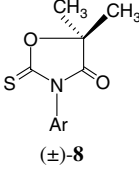
<sup>d</sup> Rate constant at coalescence temperature.

<sup>e</sup> Free energy of activation.

<sup>f</sup> The temperature at which the HPLC analysis has been done.

<sup>g</sup> The rate constant of interconversion.

**Table 3.**  $^1\text{H}$  NMR chemical shifts of *N*-*o*-tolyl substituted O, S, N containing five membered heterocyclic systems in the presence of (*S*)-TFAE. Ar = *o*-tolyl

Compound	$^1\text{H}$ NMR, ppm C-5 methyl	$^1\text{H}$ NMR, ppm <i>ortho</i> -methyl	Experimental conditions
 (±)-1	0.80 0.79 0.78	1.59 1.60	8 equiv ( <i>S</i> )-TFAE, $\text{C}_6\text{D}_6$ , 400 MHz <sup>a</sup>
 (±)-6	1.01 1.00 0.99	1.67	8 equiv ( <i>S</i> )-TFAE, $\text{C}_6\text{D}_6$ , 400 MHz
 (±)-7	1.27 1.28	1.90	8 equiv ( <i>S</i> )-TFAE, $\text{C}_6\text{D}_6$ , 200 MHz
 (±)-8	0.80 0.79 0.78	1.62	8 equiv ( <i>S</i> )-TFAE, $\text{C}_6\text{D}_6$ , 400 MHz

<sup>a</sup> Similar spectrum with 200 MHz NMR.

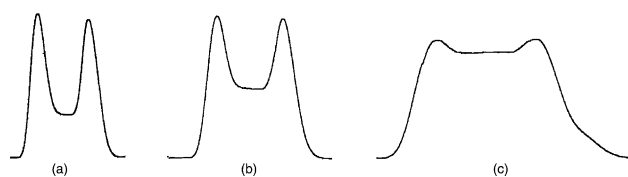


**Figure 3.** The flow rate dependent plateaus observed for (±)-5 on OD-H column, (a), flow rate = 0.3 mL/min, (b), flow rate = 0.2 mL/min, (c), flow rate = 0.1 mL/min. Eluent composition: 80:20, v/v, hexane/ethanol.

298 K) and its thermal racemization was followed by UV detection at 240 nm (Fig. 4). The barrier to rotation for the first-order interconversion process was determined using the rate constant and the Eyring equation,<sup>8</sup> and found as 94.16 kJ/mol. Data pertinent to the chromatographic separation of the enantiomers of compound (±)-5 on a Chiralpak AD column are shown in Figure 4.

We have previously found that the diastereomers of (*S*)-methyl-3-(*o*-aryl)-2,4-oxazolidinediones were obtained in unequal compositions.<sup>7</sup> The conformations of the major and the minor diastereomers were deduced from the analysis of  $^1\text{H}$  NMR, NOESY, and HMQC spectra, and it was found that the major diastereomer had a P conformation. When (*S*)-methyl-3-(*o*-iodophenyl)-2,4-oxazolidinedione, which is analogous to the compound (±)-5, was injected onto the Chiralpak AD column it was observed that the minor M conformer eluted first with eluent composition of ethanol/hexane (9:1, v/v) at a flow rate of 0.3 mL/min, at 240 nm. Since hydrogen bonding between racemic compounds and the carbamate residues of Chiralpak AD column plays an important role in chiral recognition,<sup>12</sup> and provided that these interactions are the same for the enantiomers of 5,5-dimethyl-3-(*o*-iodophenyl)-2,4-oxazolidinedione, (±)-5, and the diastereomers of (*S*)-methyl-3-(*o*-iodophenyl)-2,4-oxazolidinedione, the elution order of these compounds may be expected to be the same on the AD column, thus the first eluted enantiomer of the compound (±)-5 may correspond to the M conformer and the second to the P.

### 2.3. $^1\text{H}$ NMR in the presence of a chiral auxiliary

The chirality of compounds (±)-1–5 was also confirmed by  $^1\text{H}$  NMR spectroscopy in the presence of the chiral auxiliary (*S*)-(+)-1-(9-anthryl)-2,2,2-trifluoro ethanol [(*S*)-TFAE] (Table 1). Noncovalent interactions between the chiral auxiliary, (*S*)-TFAE, and the enantiomeric solute molecules led to the formation of diastereomeric association complexes. Hydrogen bonding between the hydroxyl group of (*S*)-TFAE and oxygen atoms of the heterocyclic ring, and  $\pi$ - $\pi$  interaction between anthryl group and benzene ring have been thought to be responsible for the formation of these association complexes.<sup>6</sup> A special type of complex formation has been proposed between lactones and (*S*)-TFAE where (*S*)-TFAE hydrogen bonds to the exocyclic oxygen with the hydroxyl proton and to the ring oxygen with the methine hydrogen.<sup>13–15</sup> The proposed structure of the complex led to the assignment of the absolute configuration of the furanone based on the consideration of different shielding effects of the anthryl group on the lactone protons.<sup>13,15</sup>

In the  $^1\text{H}$  NMR spectra of (±)-1, 3–5, the expected four singlets were observed in the presence of (*S*)-TFAE. The peaks observed with a chemical shift difference of 0.02, 0.09, 0.12, and 0.2 ppm, respectively, due to the diastereotopic methyl groups in the absence of the optically active auxiliary were found to further split by a chemical shift difference of 0.01 ppm (Table 1). Only three singlets (like triplet in appearance) were observed however for (±)-1, resulting from an accidental overlapping of two inner singlets having the same chemical shifts. *o*-Methyl protons of the two diastereomeric complexes were also observed for (±)-1 with a chemical shift difference of 0.01 ppm.

In the spectrum of (±)-2 taken in the presence of 6 equiv of (*S*)-TFAE, two singlets were observed with a chemi-

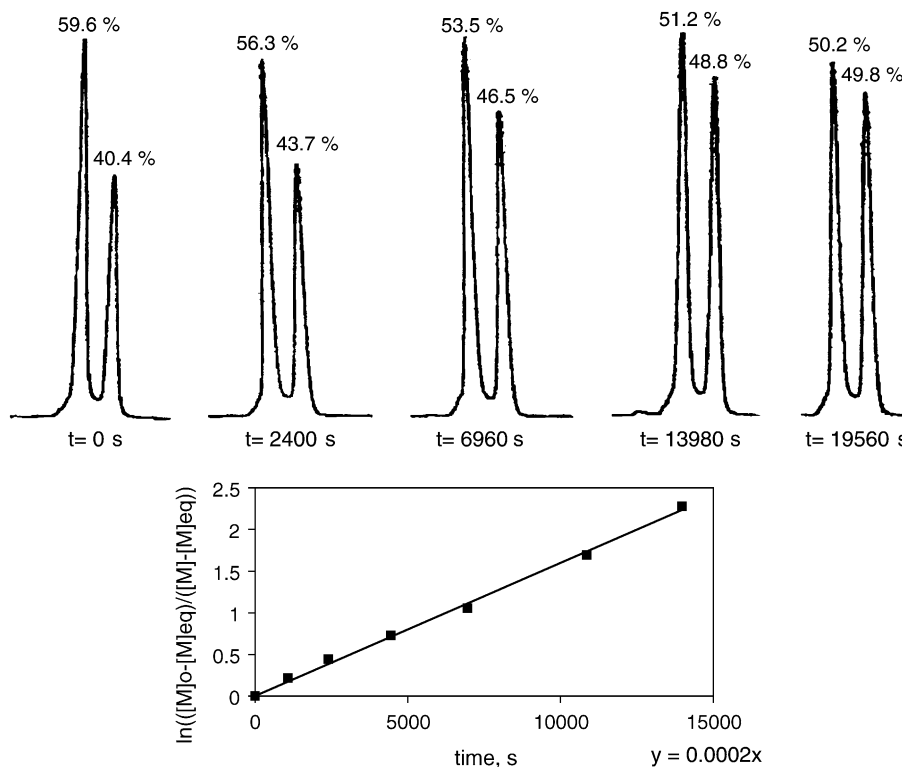


**Figure 4.** The change in enantiomer composition versus time for compound ( $\pm$ )-**5** after micropreparative enrichment of the first eluted enantiomer followed by HPLC at 293 K. Eluent: ethanol/hexane (9:1, v/v), flow rate: 0.3 mL/min,  $t_1$ : 12.85 min,  $t_2$ : 13.89 min,  $k_1$ : 0.33,  $k_2$ : 0.44,  $\alpha$ : 1.33, detection: UV at 240 nm. Inset: The plot of  $\ln(([\text{M}]_0 - [\text{M}]_{\text{eq}})/([\text{M}] - [\text{M}]_{\text{eq}}))$  versus time.

cal shift difference of 0.01 ppm due to the overlapping of two singlets because of the fast rotation around C–N single bond. In fact, when the temperature was lowered to  $-55^\circ\text{C}$ , the expected four singlets were observed.

Determination of absolute stereochemistry of certain enantiomers can be done on the basis of interactions between enantiomers and (*S*)-TFAE.<sup>15</sup> In order to get a solvation model for our compounds, all the  $^1\text{H}$  NMR signals of pure (*S*)-TFAE were compared with those of the diastereomeric association complex. It has been observed that all of the signals of the complexed anthryl, except for the hydroxyl proton, have been shielded with respect to pure (*S*)-TFAE. The downfield shift (0.1–0.2 ppm) noted for O–H proton was thought to result from hydrogen bonding with oxygens of the heterocyclic ring. Among these groups, the stronger hydrogen bonding was expected to occur between C-4 and C-2 carbonyl oxygens and the anthryl hydroxyl due to the greater basicity of these groups compared to the ring oxygen. When  $^1\text{H}$  NMR signals of enantiomers of ( $\pm$ )-**5** in the presence of (*S*)-TFAE were examined in  $\text{C}_6\text{D}_6$ , all protons were shifted upfield, probably due to the anisotropic effect of the anthryl ring. The upfield shift was also observed in  $\text{CDCl}_3$  (Table 1) ruling out the shielding effect of the solvent  $\text{C}_6\text{D}_6$ . An increase in the amount of (*S*)-TFAE also resulted in an enhancement of the shielding effect. Since an upfield shift was observed for both C-5 methyl protons of the enantiomers of ( $\pm$ )-**5**, the two-point lactone model,<sup>13–15</sup> alone cannot account for the upfield shift of both C-5 methyl protons.

A weaker  $\pi$ – $\pi$  interaction between anthryl and the *o*-substituted phenyl rings and a hydrogen bond between anthryl hydroxyl and the amide carbonyl oxygen might be the other possible interactions.<sup>13,14</sup> With the knowledge of the stereostructure of (*S*)-TFAE, in which the hydroxyl group and the carbonyl hydrogen are aligned to the same face,<sup>16,17</sup> we proposed a solvation model represented in Figure 5. In this model, while one of the phenyl rings of the anthryl system could interact with the *ortho*-substituted phenyl ring of the compounds studied the other two rings of the anthryl could not (Fig. 5).

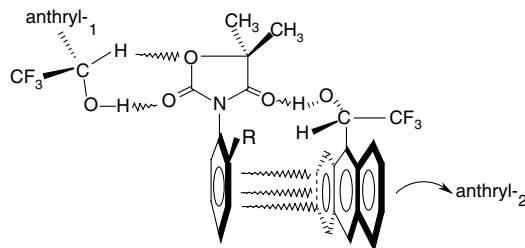


**Figure 5.** The proposed solvation model for (*M,S*) compounds ( $\pm$ )-**1–5** ( $\text{R} = \text{CH}_3, \text{F}, \text{Cl}, \text{Br}, \text{I}$ ) and (*S*)-TFAE.

In order to gain further insight for the solvation model, NOESY spectra of compound ( $\pm$ )-**5** was taken in the presence of 2 equiv of (*S*)-TFAE. Close inspection of the NOESY spectra revealed the presence of the through space  $\pi$ – $\pi$  interactions of two of the aromatic protons of

compound ( $\pm$ )-**5** and two of the anthryl protons (either protons 2, 3 or 6, 7) of (*S*)-TFAE.

The 5,5-dimethyl-3-(*o*-aryl)-2,4-oxazolidinedione enantiomers studied here are thus thought to interact with (*S*)-TFAE in three ways: (1) A two-point interaction complex is formed with the lactone part of the ring, (2) an association of the (*S*)-TFAE hydroxyl proton with the amide carbonyl oxygen and (3)  $\pi$ - $\pi$  interactions exist between the aromatic rings of the two. These interactions are schematically shown in Figure 5. The importance of the two-point lactone model in differentiation of C-5 methyl protons by NMR in the presence of (*S*)-TFAE might be confirmed when the  $^1\text{H}$  spectrum of ( $\pm$ )-**1** together with (*S*)-TFAE was compared with those of 5,5-dimethyl-3-(*o*-tolyl)-rhodanine ( $\pm$ )-**6**,<sup>6</sup> 5,5-dimethyl-3-(*o*-tolyl)-2,4-thiazolidinedione ( $\pm$ )-**7**,<sup>18</sup> and 5,5-dimethyl-3-(*o*-tolyl)-oxazolidinone-2-thione ( $\pm$ )-**8**,<sup>6</sup> in the presence of (*S*)-TFAE (Table 3). While differentiation of the C-5 methyl groups of the enantiomers of ( $\pm$ )-**1** was achieved, for ( $\pm$ )-**6** and ( $\pm$ )-**8** only one pair of the previously enantiotopic protons was distinguished in the presence of (*S*)-TFAE. The upfield pair was resolved with a chemical shift difference of 0.01 ppm whereas the downfield pair appeared as one singlet. On the other hand, for ( $\pm$ )-**7**,<sup>18</sup> only two singlets were observed instead of four. Of the *o*-methyl groups of compounds ( $\pm$ )-**1**, **6**, **7**, **8**, only those of ( $\pm$ )-**1** could be differentiated ( $\Delta\delta = 0.01$  ppm) in NMR. It can be deduced from these results that the oxygen atoms in the oxazolidinedione ring play an important role for enantiomeric discrimination in the presence of (*S*)-TFAE. As a result of lactone type of association,<sup>13–15</sup> with (*S*)-TFAE, together with association from the C-4 carbonyl oxygen and the  $\pi$ - $\pi$  interactions (Fig. 5), enantiotopic groups of the enantiomers ( $\pm$ )-**1–5** became anisochronous, thus 5,5-dimethyl protons displayed four distinct  $^1\text{H}$  NMR signals.

When  $^1\text{H}$  NMR spectrum of a mixture enriched in the M conformer of compound ( $\pm$ )-**5** was taken in the presence of (*S*)-TFAE, the chemical shifts of the diastereotopic 5,5-dimethyl protons [(a') and (b') in Fig. 6(ii)] of the (M,*S*) solvate was observed downfield to that of the (P,*S*) solvate [(a) and (b) in Fig. 6(i)]. Thus, the diastereotopic protons of the M conformer were both deshielded while those of P conformer were shielded in the presence of (*S*)-TFAE. That observation could be explained when the proposed solvate model (Fig. 5) was taken into account. Since the chemical shift differences of the diastereotopic protons [(a), (b) and (a'), (b')] of ( $\pm$ )-**5** was the same before and after the complex formation, it was thought that the difference resulted from the position of iodine atom with respect to the C-5 methyl protons. In the previous work,<sup>7</sup> we had determined by NOESY and HMQC experiments, that iodine, naphthyl and the other *ortho*-substituents, due to their anisotropy, caused a shielding effect on the protons, which had a close proximity. Therefore the protons in the upfield pair may be the ones indicated as (a) and (a'), since they were close to iodine in the P and M conformations, respectively. The discriminations of (a), (a') and (b), (b') were achieved via analysis of disposition

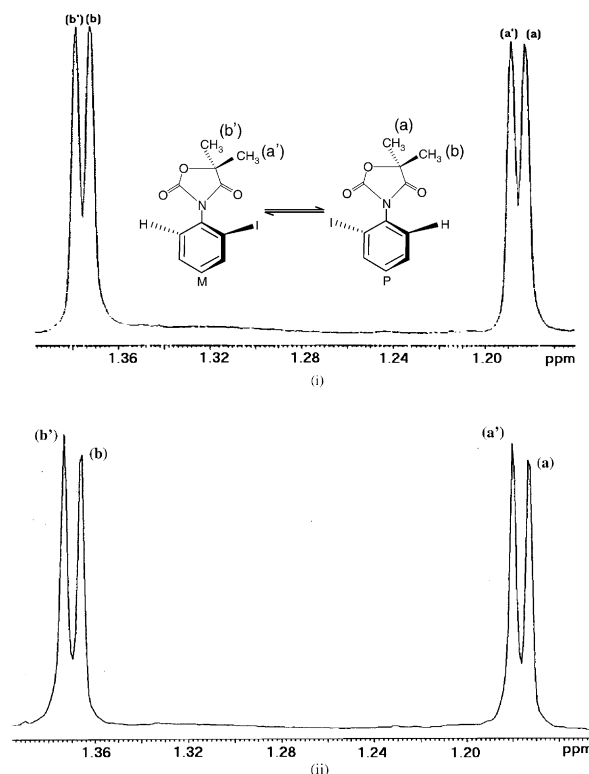


**Figure 6.** The  $^1\text{H}$  NMR signals in the presence of 8 equiv of (*S*)-TFAE in  $\text{C}_6\text{D}_6$  for the 5,5-dimethyl protons of the enantiomers ( $\pm$ )-**5**. (i) at 30 °C, (ii) at 22 °C, enriched in M conformer.

of anthryl groups. It was thought that the two anthryl groups might have slightly different anisotropic shielding effects with the closer one having the larger shielding effect.

Protons (a) and (b') were exposed to the same shielding effect by the anthryl<sub>1</sub> (Fig. 5) and they were directly included in the shielding region of this anthryl (Figs. 5 and 6). Since proton (a) unlike (b') was also shielded by the *o*-iodine it appeared as the most shielded proton. The anthryl<sub>2</sub> might have an important role in the shielding of (a') and (b). This anthryl group may have had a tighter approach for the (P,*S*) solvate than for the (M,*S*) solvate,<sup>19</sup> owing to the steric interaction of the lone pair electrons of the *o*-iodine in the M conformer and the  $\pi$  electrons of the anthryl group,<sup>13</sup> which prevented the two rings being close to each other. Therefore, by virtue of the greater proximity of the proton (b) to anthryl<sub>2</sub> group than the proton (b') to anthryl<sub>1</sub>, the proton (b) of the P conformer may experience a stronger shielding effect than the proton (b') of M conformer. The proton (a') was affected by *o*-iodine together with anthryl<sub>2</sub>, therefore it was shielded to the upfield region. On the other hand, shielding of (a') by anthryl<sub>2</sub> was not as strong as that of (a) by anthryl<sub>1</sub> because of the prevention of a tight complex by *o*-iodine in the M conformer.

Since the *ortho*-substituents are known to have a shielding effect on the *syn*-substituent at C-5,<sup>7</sup> it can be argued that of all the compounds studied, ( $\pm$ )-**1–5**, in the presence of (*S*)-TFAE the more deshielded of the diastereo-

topic 5-methyl pairs can be assigned to the complexed M conformer and the more shielded to complexed P.

### 3. Conclusion

The activation barriers for 5,5-dimethyl-3-(*o*-tolyl)-2,4-oxazolidinedione, 5,5-dimethyl-3-(*o*-fluorophenyl)-2,4-oxazolidinedione, 5,5-dimethyl-3-(*o*-chlorophenyl)-2,4-oxazolidinedione and 5,5-dimethyl-3-(*o*-bromophenyl)-2,4-oxazolidinedione were determined as 73.49, 57.33, 83.06, and 86.44 kJ/mol, respectively, by temperature dependent NMR.

The enantiomers of 5,5-dimethyl-3-(*o*-iodophenyl)-2,4-oxazolidinedione were resolved micro-preparatively on Chiralpak AD. The thermal racemization of the enriched enantiomer was followed to obtain the barrier to rotation, which amounted to 94.16 kJ/mol.

The activation energies showed a linear increase with the van der Waals radii of the *ortho*-halogen substituents.

A diastereomeric association model between the enantiomers of 5,5-dimethyl-3-(*o*-aryl)-2,4-oxazolidinedione and the chiral auxiliary (*S*)-TFAE has been drawn. The conformational assignments of the enantiomers were achieved via this solvation model, on the basis of the relative chemical shift values of the well resolved four singlets of the C-5 methyl protons in the presence of (*S*)-TFAE. This solvation model fitted well with the absolute conformations predicted by comparison of the elution orders in enantioselective HPLC of the structurally related compounds whose absolute stereostructures had been determined before.

### 4. Experimental

<sup>1</sup>H and <sup>13</sup>C NMR spectra of all compounds were recorded on a Varian-Mercury VX-400 MHz-BB (30 °C) or Bruker AC-200L (200 MHz, 22 °C). IR analyses were performed on a Mattson Genesis II FTIR using KBr discs for 2,4-oxazolidinedione derivatives and NaCl windows for *o*-aryl isocyanates. Chromatographic analyses were done using Cecil 1100 pump (*P* = 3–3.5 Mpa), a Rheodyne, 7125 injector mode with a 20 μL sample loop, a Cecil UV monitor (240 nm) and an integrating recorder. The chiral columns used were commercially available Chiralcel OD-H (4.6 mm ID × 250 mm L, 5 μm, Daicel, Tokyo, Japan) and Chiralpak AD (4.6 mm ID × 250 mm L, 5 μm, Daicel,

Tokyo, Japan). Thermohypersil-Keystone column pocket was used for the temperature control of the Chiralpak AD column. Elemental analyses were performed on Carlo Erba 1106. Melting points were recorded using Electrothermal 9100 melting point apparatus.

#### 4.1. Syntheses

The compounds, (±)-**1–5**, 5,5-dimethyl-3-(*o*-aryl)-2,4-oxazolidinediones were synthesized by the reaction of ethyl α-hydroxyisobutyrate and *o*-aryl isocyanates in the presence of sodium metal in toluene (Fig. 7).<sup>7</sup>

**4.1.1. General procedure.** In a 100 mL three-necked flask, fitted with a thermometer and reflux condenser, *o*-aryl isocyanate and ethyl α-hydroxyisobutyrate were mixed in toluene. Sodium metal was added prior to heating in small pieces. After the addition of sodium, the mixture was heated for 10 h at about 80 °C then the temperature was raised to 100–110 °C for 1 h. At the end of the reflux process, dark-orange crude products were obtained. After dissolving in ethanol, 5,5-dimethyl-3-(*o*-aryl)-2,4-oxazolidinediones separated as white crystals. The compounds were further purified by recrystallization from ethanol and identified based on their <sup>1</sup>H NMR spectra and elemental analyses.

*o*-Aryl isocyanates used as starting materials were synthesized by the reaction of the corresponding acid chloride with sodium azide by the Curtius rearrangement of the acyl azide.<sup>7</sup> The isocyanates were identified by their IR spectra.

#### 4.1.2. 5,5-Dimethyl-3-(*o*-tolyl)-2,4-oxazolidinedione (±)-**1**.

The compound was prepared according to the general procedure using 3.87 g (0.029 mol) ethyl α-hydroxyisobutyrate, 3.90 g (0.029 mol) *o*-tolyl isocyanate, 0.12 g (0.0052 mol) sodium metal and 15 mL toluene. Yield: 3.28 g, 51.6%. Mp 91.2–92.2 °C. <sup>1</sup>H NMR (200 MHz) data in C<sub>6</sub>D<sub>6</sub>: diastereotopic methyl protons at C-5: δ = 1.15 ppm (s, 3H), 1.17 ppm (s, 3H). *o*-Methyl protons: δ = 1.97 ppm (s, 3H). Aromatic protons: δ = 6.88–7.03 ppm (m, 4H). <sup>13</sup>C NMR data in C<sub>6</sub>D<sub>6</sub>: carbonyl carbons in the heterocyclic ring: 174.8, 153.1 ppm. Diastereotopic methyl carbons: 23.0, 23.7 ppm. Methine carbon (C-5) in the heterocyclic ring: 83.5 ppm. *o*-Methyl carbon: 17.4 ppm. Aromatic carbons: 127.1, 128.54, 129.8, 130.5, 131.3, 136.2 ppm. Elemental analysis data: Found: C, 64.61; H, 5.93; N, 5.57%. Calcd for C<sub>12</sub>H<sub>13</sub>O<sub>3</sub>N: C, 65.74; H, 5.98; N, 6.39%. IR data: ν<sub>Ar-H</sub>:

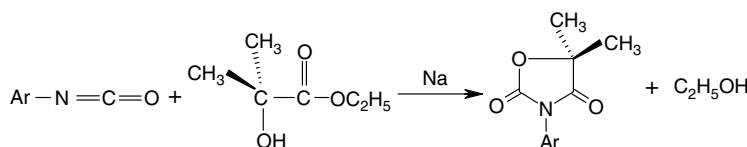


Figure 7. The synthesis of 5,5-dimethyl-3-(*o*-aryl)-2,4-oxazolidinediones.

3066 cm<sup>-1</sup>, aromatic C–H stretching;  $\nu_{\text{C-H}}$ : 2985, 2934, 2875 cm<sup>-1</sup>, alkyl C–H stretching;  $\nu_{\text{C=O}}$ : 1749 cm<sup>-1</sup>, carbonyl stretching;  $\nu_{\text{C-H}}$ : 1498, 1463, 1405 cm<sup>-1</sup>, alkyl C–H bending;  $\nu_{\text{C-H}}$ : 767 cm<sup>-1</sup>, *o*-disubstituted aromatic C–H out-of-plane bending;  $\nu_{\text{C-O}}$ : 1173 cm<sup>-1</sup>, –C–O stretching.

**4.1.3. 5,5-Dimethyl-3-(*o*-fluorophenyl)-2,4-oxazolidinedione (±)-2.** The compound was prepared according to the general procedure using 2.06 g (0.015 mol) *o*-fluorophenyl isocyanate, 1.98 g (0.015 mol) ethyl  $\alpha$ -hydroxyisobutyrate, 0.03 g (0.0013 mol) sodium metal and 15 mL toluene. Yield: 1.17 g, 34.7%. Mp 114.1–114.8 °C. <sup>1</sup>H NMR (200 MHz) data in C<sub>6</sub>D<sub>6</sub>: Diastereotopic methyl protons at C-5:  $\delta$  = 1.11 ppm (s, 6H). Aromatic protons:  $\delta$  = 6.60–7.48 ppm (m, 4H). <sup>13</sup>C NMR data in C<sub>6</sub>D<sub>6</sub>: Carbonyl carbons in the heterocyclic ring: 174.2, 160.5, 155.4, 152.4 ppm. Diastereotopic carbons at C-5: 23.3 ppm. Aromatic carbons: 124.8, 125.7, 129.2, 129.6, 131.3, 131.4, 116.9, 116.5 ppm. Elemental analysis data: Found: C, 59.78; H, 4.84; N, 6.33%. Calcd for C<sub>11</sub>H<sub>10</sub>O<sub>3</sub>NF: C, 59.19; H, 4.54; N, 6.28%. IR data:  $\nu_{\text{Ar-H}}$ : 3078 cm<sup>-1</sup>, aromatic C–H stretching;  $\nu_{\text{C-H}}$ : 2992, 2942 cm<sup>-1</sup>, alkyl C–H stretching;  $\nu_{\text{C=O}}$ : 1744 cm<sup>-1</sup>, carbonyl stretching;  $\nu_{\text{C-H}}$ : 1508, 1410 cm<sup>-1</sup>, alkyl C–H bending;  $\nu_{\text{C-H}}$ : 774 cm<sup>-1</sup>, *o*-disubstituted aromatic C–H out-of-plane bending;  $\nu_{\text{C-O}}$ : 1170 cm<sup>-1</sup>, –C–O stretching.

**4.1.4. 5,5-Dimethyl-3-(*o*-chlorophenyl)-2,4-oxazolidinedione (±)-3.** The compound was prepared according to the general procedure using 1.54 g (0.01 mol) *o*-chlorophenyl isocyanate, 1.32 g (0.01 mol) ethyl  $\alpha$ -hydroxyisobutyrate, 0.023 g (0.001 mol) sodium metal and 15 mL toluene. Yield: 0.58 g, 24.3%. Mp 94.9–95.6 °C. <sup>1</sup>H NMR (200 MHz) data in C<sub>6</sub>D<sub>6</sub>: diastereotopic methyl protons at C-5:  $\delta$  = 1.16 ppm (s, 3H), 1.25 ppm (s, 3H). Aromatic protons:  $\delta$  = 6.60–7.00 ppm (m, 4H). <sup>13</sup>C NMR data in C<sub>6</sub>D<sub>6</sub>: carbonyl carbons in the heterocyclic ring: 174.2, 152.3 ppm. Diastereotopic methyl carbons at C-5: 22.9, 23.8 ppm. Methine carbon (C-5) in the heterocyclic ring: 84.1 ppm. Aromatic carbons: 127.8, 129.2, 130.4, 131.1, 132.9 ppm. Elemental analysis data: Found: C, 53.94; H, 4.14; N, 4.99%. Calcd for C<sub>11</sub>H<sub>10</sub>O<sub>3</sub>NCl: C, 55.13; H, 4.21; N, 5.84%. IR data:  $\nu_{\text{C-H}}$ : 2987 cm<sup>-1</sup>, alkyl C–H stretching;  $\nu_{\text{C=O}}$ : 1745 cm<sup>-1</sup>, carbonyl stretching;  $\nu_{\text{C-H}}$ : 1488, 1406 cm<sup>-1</sup>, alkyl C–H bending;  $\nu_{\text{C-H}}$ : 772 cm<sup>-1</sup>, *o*-disubstituted aromatic C–H out-of-plane bending;  $\nu_{\text{C-O}}$ : 1171 cm<sup>-1</sup>, –C–O stretching.

**4.1.5. 5,5-Dimethyl-3-(*o*-bromophenyl)-2,4-oxazolidinedione (±)-4.** The compound was prepared according to the general procedure using 1.98 g (0.01 mol) *o*-bromophenyl isocyanate, 1.32 g (0.01 mol) ethyl  $\alpha$ -hydroxyisobutyrate, 0.02 g (0.00087 mol) sodium metal and 15 mL toluene. Yield: 1.24 g, 43.7%. Mp 91.7–92.4 °C. <sup>1</sup>H NMR (200 MHz) data in C<sub>6</sub>D<sub>6</sub>: Diastereotopic methyl protons at C-5:  $\delta$  = 1.2 ppm (s, 3H), 1.3 ppm (s, 3H). Aromatic protons:  $\delta$  = 6.5–7.2 ppm (m, 4H). <sup>13</sup>C NMR data in C<sub>6</sub>D<sub>6</sub>: carbonyl carbons in the heterocyclic ring: 174.1, 152.3 ppm. Diastereotopic methyl carbons at C-5:

22.9, 23.8 ppm. Methine carbon (C-5) in the heterocyclic ring: 84.2 ppm. Aromatic carbons: 122.9, 128.6, 129.2, 130.5, 131.4, 133.5 ppm. Elemental analysis data: Found: C, 46.78; H, 3.79; N, 4.61%. Calcd for C<sub>11</sub>H<sub>10</sub>O<sub>3</sub>NBr: C, 46.5; H, 3.55; N, 4.93%. IR data:  $\nu_{\text{Ar-H}}$ : 3067 cm<sup>-1</sup>, aromatic C–H stretching;  $\nu_{\text{C-H}}$ : 2986, 2937 cm<sup>-1</sup>, alkyl C–H stretching;  $\nu_{\text{C=O}}$ : 1749 cm<sup>-1</sup>, carbonyl stretching;  $\nu_{\text{C-H}}$ : 1485, 1411 cm<sup>-1</sup>, alkyl C–H bending;  $\nu_{\text{C-H}}$ : 763 cm<sup>-1</sup>, *o*-disubstituted aromatic C–H out-of-plane bending;  $\nu_{\text{C-O}}$ : 1180 cm<sup>-1</sup>, –C–O stretching.

**4.1.6. 5,5-Dimethyl-3-(*o*-iodophenyl)-2,4-oxazolidinedione (±)-5.** The compound was prepared according to the general procedure using 1.59 g (6.5 × 10<sup>-3</sup> mol) *o*-iodophenyl isocyanate, 0.86 g (6.5 × 10<sup>-3</sup> mol) ethyl  $\alpha$ -hydroxyisobutyrate, 0.015 g (6.5 × 10<sup>-4</sup> mol) sodium metal and 15 mL toluene. Yield: 0.87 g, 40.4%. Mp 118.2–119.2 °C. <sup>1</sup>H NMR (400 MHz) data in C<sub>6</sub>D<sub>6</sub>: diastereotopic methyl protons at C-5:  $\delta$  = 1.2 ppm (s, 3H), 1.4 ppm (s, 3H). Aromatic protons:  $\delta$  = 6.4–7.4 ppm (m, 4H). <sup>13</sup>C NMR data in C<sub>6</sub>D<sub>6</sub>: carbonyl carbons in the heterocyclic ring: 172.1 ppm, 150.3 ppm. Diastereotopic methyl carbons at C-5: 21.8, 22.4 ppm. Methine carbon (C-5) in the heterocyclic ring: 82.4 ppm. Aromatic carbons: 127.7, 128.1, 129.5, 132.6, 138.2. Elemental analysis data: Found: C, 39.91; H, 2.99; N, 3.86%. Calcd for C<sub>11</sub>H<sub>10</sub>O<sub>3</sub>NBr: C, 39.9; H, 3.00; N, 4.23%. IR data:  $\nu_{\text{Ar-H}}$ : 3070 cm<sup>-1</sup>, aromatic C–H stretching;  $\nu_{\text{C-H}}$ : 2933, 2984 cm<sup>-1</sup>, alkyl C–H stretching;  $\nu_{\text{C=O}}$ : 1746 cm<sup>-1</sup>, carbonyl stretching;  $\nu_{\text{C-H}}$ : 1405, 1477 cm<sup>-1</sup>, alkyl C–H bending;  $\nu_{\text{C-H}}$ : 767 cm<sup>-1</sup>, *o*-disubstituted aromatic C–H out-of-plane bending;  $\nu_{\text{C-O}}$ : 1176 cm<sup>-1</sup>, –C–O stretching.

### Acknowledgements

This project has been supported by Boğaziçi University research fund (BAP) with project number 03B503.

### References and notes

- Walker, R. B.; Fitz, L. D.; Williams, L. M.; Linton, H.; Smith, C. C. *Gen. Pharmacol.: Vascular Syst.* **1993**, *24*, 669–673.
- Momose, Y.; Maekawa, T.; Yamano, T.; Kawada, M.; Odaka, H.; Ikeda, H.; Sohda, T. *J. Med. Chem.* **2002**, *45*, 1518–1534.
- Lin, G. Q.; Li, Y. M.; Chan, A. S. C. *Principles and Applications of Asymmetric Synthesis*; Wiley Interscience: New York, 2001. pp 135–188.
- Aitken, R. A.; Kilenyi, S. N. *Asymmetric Synthesis*; Blackie Academic & Professional: London, 1992. pp 83–140.
- Shapiro, S. L.; Rose, I. M.; Testa, F. C.; Roskin, E.; Freedman, L. *J. Am. Chem. Soc.* **1959**, *81*, 6498–6504.
- Doğan, İ.; Burgemeister, T.; İçli, S.; Mannschreck, A. *Tetrahedron* **1992**, *48*, 7157–7164.
- Demir, Ö.; Doğan, İ. *Chirality* **2003**, *15*, 242–250.

8. Alberty, R. A.; Silbey, R. J. *Physical Chemistry*; Wiley: New York, 1992.
9. Bürkle, W.; Karfunkel, H.; Schurig, V. *J. Chromatogr.* **1984**, *288*, 1–14.
10. Mannschreck, A.; Kiebi, L. *Chromatographia* **1989**, *28*, 263–266.
11. Wolf, C.; Pirkle, W. H.; Welch, C. J.; Hochmuth, D. H.; König, W. A.; Chee, G. L.; Charlton, J. L. *J. Org. Chem.* **1997**, *62*, 5208–5210.
12. Okamoto, Y.; Kaida, Y. *J. Chromatogr. A* **1994**, *666*, 403–419.
13. Pirkle, W. H.; Sikkenga, D. L. *J. Org. Chem.* **1977**, *42*, 1370–1374.
14. Allinger, N. L.; Eliel, E. L.; Wilen, S. H. *Topics in Stereochemistry*; John Wiley & Sons: New York, 1982; pp 263–331.
15. Jullian, J. C.; Franck, X.; Latypov, S.; Hocquemiller, R.; Figadere, B. *Tetrahedron: Asymmetry* **2003**, *14*, 963–966.
16. Pirkle, W. H.; Finn, J. M. *J. Org. Chem.* **1981**, *46*, 2935–2938.
17. Lipkowitz, K. B.; Demeter, D. A.; Parish, C. A. *Anal. Chem.* **1987**, *59*, 1733–1736.
18. Karataş, M.; Koni, S.; Doğan, İ. *Can. J. Chem.* **1998**, *76*, 254–259.
19. Beaufour, M.; Merelli, B.; Menguy, L.; Cherton, J. C. *Chirality* **2003**, *15*, 382–390.